Self-Interference Flow of an Isotactic Polypropylene Melt in a Cavity during Injection Molding. I. Effect of the Self-Interference Flow on the Properties

Wenli Dai, Pengsheng Liu, Xiayu Wang

College of Chemistry, Xiangtan University, Hunan 411105, China

Received 30 January 2002; accepted 3 September 2002

ABSTRACT: The self-interference flow (SIF) of a melt in a cavity during injection molding is introduced. It comes from two streams of the melt being split by a patented mold gate called a twin gate. The effects of this flow on the static and dynamic mechanical properties, thickness distribution, and shrinkage in the transverse direction (TD) of injection-molded isotactic polypropylene parts are discussed. SIF has an influence on the static mechanical properties, especially the impact strength. There are slight increases in the tensile strength and Young's modulus and an increase of approximately 70–90% in the impact strength in comparison with the properties of samples obtained by a conventional flow process with a common pin gate. Dynamic mechanical thermal analysis studies show an increase in the storage modulus for SIF samples. Results obtained from research into the effect of the mold temperature and injection pressure on the impact strength show that the impact strength of SIF specimens has a weaker dependence on the mold temperature and injection pressure. In addition, the flow brings a more uniform thickness distribution and a smaller shrinkage in the TD to SIF samples. © 2003 Wiley Periodicals, Inc. J Appl Polym Sci 88: 2784–2790, 2003

Key words: isotactic polypropylene (iPP); injection molding; mechanical properties

INTRODUCTION

Injection molding can shape a part with an insert (or many inserts) or a complex figure, and it is adaptable to almost all kinds of thermoplastics; therefore, it is widely applied in the plastics manufacturing industry. However, some defects, such as weld lines, warpage, sink marks, and low accuracy and strength, are still found in parts made in this way. To overcome these defects, particularly the low accuracy and strength, researchers have worked on moldings in three ways. First, they have sought the optimum molding parameters for a material. Although this can result in the modification of the properties of the molded part, the modification is often slight and not quantified.[1] Recent studies have been focused on the relationship between the processing parameters and the properties so that the part quality can be controlled by means of a computer.[2–4] Second, researchers have improved the properties of the material. Simple and useful ways for doing this include blending, compounding, and copolymerization, and there are many reports about these.[5–10] Third, researchers have made innovations in the molding process by means of additional devices. This is a hot topic now. This study is focused on vibration technology, by which researchers[1,11–16] have made progress in the properties of molded parts. For example, Guan et al.[11] reported that the tensile strength of isotactic polypropylene (iPP) was enhanced from the original value of 31.0 MPa to 57.8 MPa by oscillating packing injection molding under low pressure, and Kalay and Bevis[12] reported that the impact strength was increased four times by shear-controlled injection molding.

The aim of this two-part series is to present a way of modifying injection-molded iPP parts through changes in the mold structure. We used a patented mold gate,[17] called a twin gate, to make the melt in the cavity produce self-interference actions to form a specific morphology, which, to a large extent, controlled the properties. In this article, we discuss the mechanical properties and dimensional variations of the moldings, which were injection-molded under the condition of self-interference flow (SIF) generated by the twin gate with various parameters, and we compare the results with those obtained by a conventional flow process (CFP) with a common pin gate. In the second article of this series, we discuss the morphology of the moldings and reveal the relationship of the microstructure of the SIF samples to their properties.

Correspondence to: W. Dai (daiwenlp@xtu.edu.cn).

Journal of Applied Polymer Science, Vol. 88, 2784–2790 (2003)

TABLE I
Main Processing Parameters in This Experiment

Injection pressure (MPa)	Dwelling time (s)	Mold-temperature (°C)	Injection rate (cm^3/s)
45	1	30	10
55	4	40	10
65	7	50	10
75	10	60	10
85	13	70	10

EXPERIMENTAL

Sample preparation

The iPP used in this study was J300 (melt index = 5.5 g/10 min) from Beijing Yanshan Petrochemical Co. (China). The injection-molding experiments were performed on an HTB80 machine with a 35-mm-diameter screw; the maximum injection volume was 125 cm^3, and the maximum clamping force was 800 kN. The injection-molding process was program-controlled. Temperature controls on the barrel included three heat-control zones; along the direction of the conveying material, the temperatures of the three zones were 190, 210, and 230°C. A mold-temperature adjuster controlled the temperature of the mold platens with circulating water. The main parameters are summarized in Table I.

A two-cavity mold was employed, one equipped with a conventional pin gate and the other equipped with a twin gate, each being a rectangular slab (100 mm × 60 mm × 4 mm). For simplicity, the runner and gates were designed on the part face, with their cross section being semiround. The section areas of the two gates were equal; that is, the area of the pin gate was equal to the addition of the two orifices of the twin gate. Figure 1 illustrates the structure of the twin gate used in this study, which consisted of two orifices sharing the same runner. After the slabs were obtained, they were cut into the specimens required for the test. The procedure is illustrated in Figure 2.

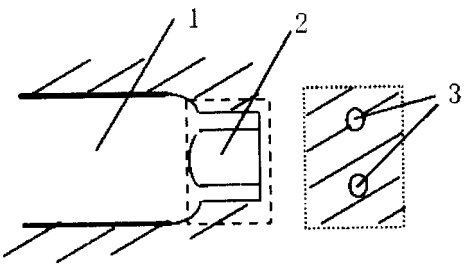

Figure 1 Illustration of the twin-gate structure: (1) the runner, (2) the twin gate, and (3) the two orifices in the twin gate.

Tensile testing

An Instron universal testing machine (model 5500, USA) was used for tensile testing at room temperature (23°C); the crosshead speed was 50 mm/min.

Impact strength

Notched charpy impact strength values were measured by means of a charpy impact machine (model

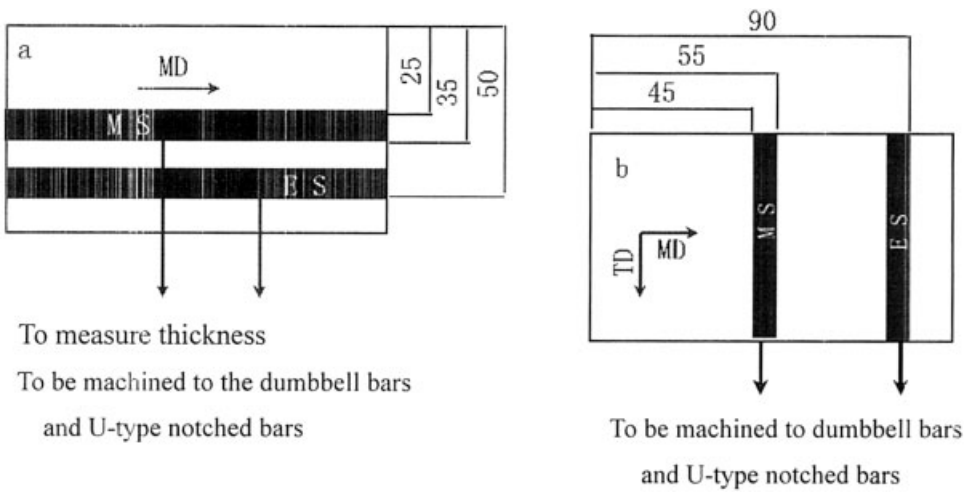

Figure 2 Procedure for making (a) specimens cut in the MD and (b) specimens cut in the TD.

XJ-5, Chengde Precision Tester Co., China) according to GB/T1043-93.

Dynamic mechanical thermal analysis (DMTA)

Dynamic mechanical tests were carried out with a Netzsh DMA242 instrument (Germany) at a frequency of 1 Hz and a heating rate of 3°C/min from −50 to 150°C. Samples were cut from the middle-sample (MS) specimens in the machine direction (MD).

Dimensional stability

The sample thickness was measured with a micrometer with an accuracy of 0.001 mm, and the sample width was measured with a micrometer dial with an accuracy of 0.001 mm. The shrinkage was tested in line with ASTM D 955. Each data point represents the mean of values obtained for least five specimens.

RESULTS AND DISCUSSION

SIF

The importance of the flow pattern during mold filling in determining the details of the microstructure and, therefore, the properties, is considerable. The flow pattern in an advancing front between two parallel plates was reported by Tadmor,[18] and the pattern during conventional injection molding was described in detail by Han.[19] Katti and Schultz[20] gave a schematic of the pattern for a rectangular cross-sectioned cavity and separated the progression of the flow front into three stages. In stage I, the flow front was semicircular; in stage II, the flow front was shaped as an arc of circle, and the angle of the arc decreased as time increased; and in stage III, the flow front was complex as the corners of the cavity were filled. We have discussed the flow pattern of the melt that passes through the twin gate into the cavity through an investigation of samples with volumes one-fifth, one-fourth, and two-thirds of the cavity prepared by short shot.[21] In light of the experimental phenomena, a flow pattern in the cavity, called SIF, is proposed. Figure 3 shows how to form SIF of the melt in the cavity by means of the twin gate during injection molding. When a melt flows through orifices 1 and 2 successively, their flow patterns [Fig. 3(a,b)] in the cavity are similar to those when a melt flows through a pin gate (i.e., a CFP).[20] However, when a melt passes through orifices 1 and 2 at the same time (i.e., a twin gate), interactions between the two streams of the melt split by the gate take place: they overlap each other in the MD [Fig. 3(c′)], with this resulting in a melt front [Fig. 3(c)], but they collide with each other in the transverse direction [TD; Fig. 3(c′)], with this leading to a trend of melt flowing, that is, a transverse flow. The interference actions are caused only under an injection pressure, without any other forces, and so we call this kind of melt flow in a cavity SIF.

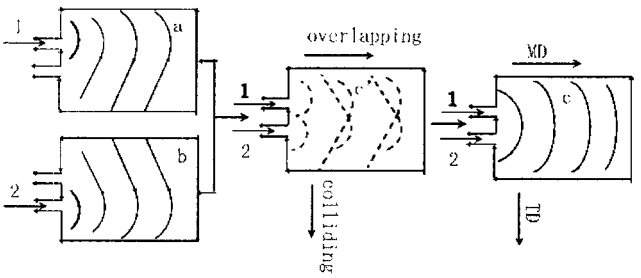

Figure 3 Illustration of the SIF mechanism: (a,b) a flow sketch of the melt passing through orifices 1 and 2, respectively, and (c′,c) a flow sketch of the melt passing through orifices 1 and 2 at the same time (a twin gate).

Mechanical properties

With a dwelling time of 4 s and an injection rate of 10 cm^3/s and for various injection pressures and mold temperatures, the testing results are listed in Tables II and III for the MS specimens and in Tables IV and V for the edge-sample (ES) specimens. In general, for the SIF and CFP specimens, in either the MD or TD, when

TABLE II
Mechanical Properties of the MS Specimens with Variations in the Injection Pressure (4-s Dwelling Time, 40°C Mold Temperature)

Sample	Injection pressure (MPa)	Tensile strength (MPa)		Young's modulus (GPa)		Impact strength (kJ/m^2)	
		MD	TD	MD	TD	MD	TD
CFP	55	31.02	30.07	1.36	1.29	2.17	2.12
	65	33.51	31.69	1.38	1.31	2.11	2.01
	85	36.33	34.83	1.53	1.47	1.87	1.72
Mean standard deviations		1.05	1.02	0.11	0.12	0.14	0.14
SIF	55	31.47	30.85	1.34	1.30	3.75	3.73
	65	33.82	33.94	1.48	1.46	3.78	3.76
	85	36.35	35.13	1.61	1.55	3.54	3.54
Mean standard deviations		1.01	1.03	0.11	0.11	0.12	0.12

TABLE III
Mechanical Properties of the MS Specimens with Variations in the Mold Temperature (55-MPa Injection Pressure, 4-s Dwelling Time)

Sample	Mold temperature (°C)	Tensile strength (MPa)		Young's modulus (GPa)		Impact strength (kJ/m^2)	
		MD	TD	MD	TD	MD	TD
CFP	40	31.02	30.07	1.36	1.29	2.17	2.12
	50	33.83	32.74	1.51	1.46	2.05	1.94
	70	37.51	36.17	1.71	1.69	1.82	1.81
Mean standard deviations		1.10	1.07	0.12	0.12	0.13	0.13
SIF	40	31.47	30.85	1.34	1.30	3.75	3.73
	50	34.11	33.18	1.53	1.52	3.76	3.72
	70	37.49	36.43	1.74	1.69	3.31	3.17
Mean standard deviations		1.08	1.06	0.09	0.12	0.10	0.13

the injection pressure or mold temperature is raised, the tensile strength and Young's modulus show an increasing trend, and the values of the SIF specimens are a little higher than those of CFP specimens under the same conditions. The tensile strength and Young's modulus increase with the mold temperature because the degree of crystallinity increases with the mold temperature.[16,22] The effect of the injection pressure on the tensile strength and Young's modulus can be explained simply by the Clapeyron equation, which predicts a linear increase of T_m with pressure. As T_m increases with pressure, so does the degree of supercooling, $T_{m(p)} - T_c$, and this favors the increase in the crystallinity. From Tables II–V, we can also observe other distinguishing features brought about by melt self-interference actions:

1. For SIF specimens, the impact strength is improved. There is about a 70–90% increase in the impact strength both in the MD and in the TD, and this undoubtedly results from the interference flow of the melt.

TABLE IV
Mechanical Properties of the ES Specimens with Variations in the Injection Pressure (4-s Dwelling Time, 40°C Mold Temperature)

Sample	Injection pressure (MPa)	Tensile strength (MPa)		Young's modulus (GPa)		Impact strength (kJ/m^2)	
		MD	TD	MD	TD	MD	TD
CFP	55	29.31	28.12	1.32	1.27	2.34	2.47
	65	31.84	29.91	1.35	1.31	2.12	2.30
	85	36.03	34.34	1.51	1.42	2.08	2.16
Mean standard deviations		1.03	1.03	0.09	0.08	0.10	0.11
SIF	55	31.06	29.34	1.32	1.30	3.78	3.85
	65	33.17	32.16	1.42	1.33	3.78	3.87
	85	36.79	35.28	1.59	1.37	3.61	3.70
Mean standard deviations		1.06	1.01	0.10	0.09	0.10	0.07

TABLE V
Mechanical Properties of the ES Specimens with Variations in the Mold Temperature (55-MPa Injection Pressure, 4-s Dwelling Time)

Sample	Mold temperature (°C)	Tensile strength (MPa)		Young's modulus (GPa)		Impact strength (kJ/m^2)	
		MD	TD	MD	TD	MD	TD
CFP	40	29.31	28.12	1.32	1.27	2.34	2.47
	50	33.07	31.75	1.47	1.36	2.10	2.13
	70	36.81	35.93	1.68	1.50	1.92	1.97
Mean standard deviations		1.08	1.02	0.13	0.09	0.09	0.11
SIF	40	31.06	29.34	1.32	1.30	3.78	3.85
	50	34.07	32.64	1.42	1.33	3.79	3.91
	70	37.20	36.28	1.69	1.59	3.53	3.55
Mean standard deviations		1.10	1.03	0.13	0.10	0.09	0.09

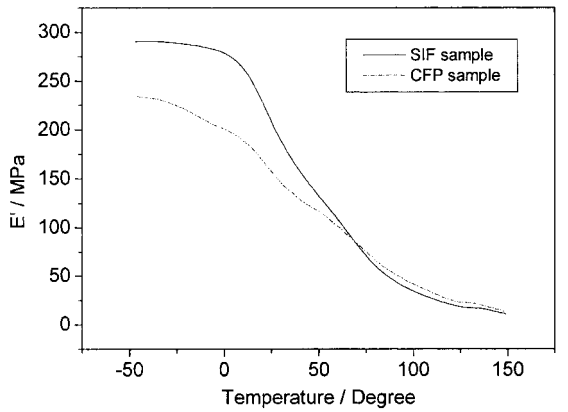

Figure 4 E' versus temperature.

2. For CFP specimens, either in the MD or in the TD, the impact strength decreases with an increase in the mold temperature or injection pressure, but for SIF specimens, the impact strength changes a little, showing a weaker dependence on the mold temperature and injection pressure.

Figure 4 shows the temperature dependence of the dynamic storage modulus (E') for the SIF and CFP samples. It is obvious that the SIF sample exhibits a higher value of E' than the CFP sample until about 60°C. The maximum increment is about 40%. Therefore, SIF is also conducive for increasing E'.

Shrinkage

Figures 5–7 show the effects of the dwelling time, injection pressure, and mold temperature, respectively, on shrinkage in the TD. Looking at these figures, we can observe that the shrinkage of the SIF samples is smaller than that of the CFP specimens under the same conditions, regardless of the change in the dwelling time, injection pressure, and mold temperature. This results from SIF of the melt in the cavity, particularly the transverse flow. Figure 5 also demonstrates that when a constant shrinkage occurs, for the pin gate, the dwelling time is up to 11 s, but for the twin gate, the dwelling time is about 7 s. This means that the freezing time of the twin gate is shorter. Besides, the shrinkage for either SIF specimens or CFP specimens increases with the mold temperature but decreases with an increase in the injection pressure and dwelling time. This conclusion corresponds with the conclusions of other works.[23–25]

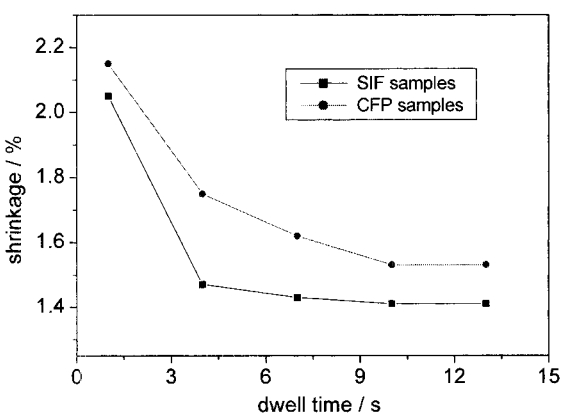

Figure 5 Effect of the dwelling time on the shrinkage of the twin-gate and pin-gate samples at a mold temperature of 40°C and an injection pressure of 55 MPa.

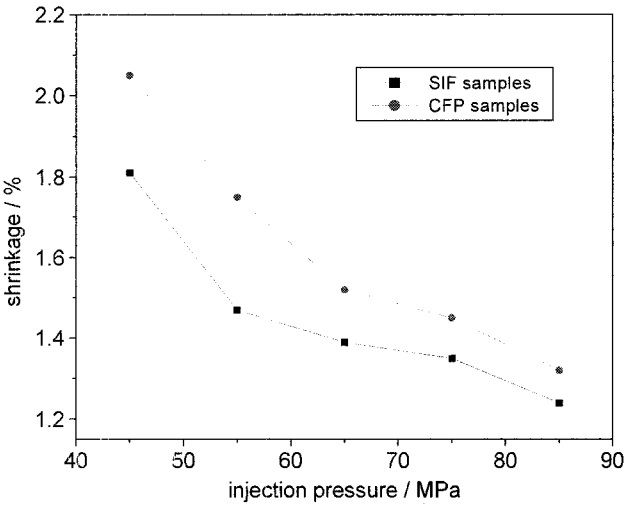

Figure 6 Effect of the injection pressure on the shrinkage of the twin-gate and pin-gate samples at a mold temperature of 40°C and a dwelling time of 4 s.

Thickness distribution

We measured the thickness distribution along the MD and compared the distribution of the SIF samples with

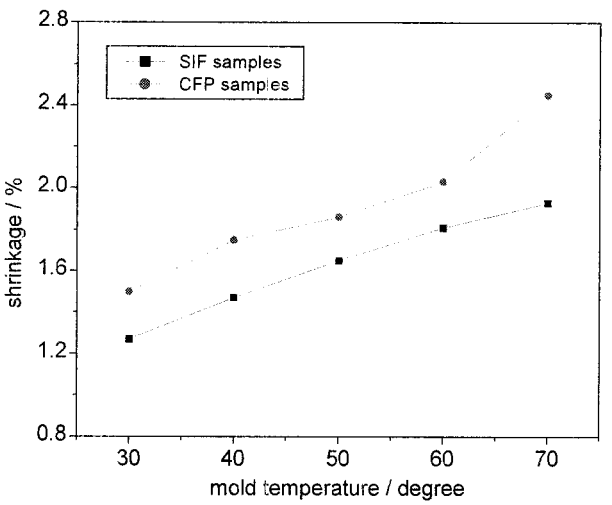

Figure 7 Effect of the mold temperature on the shrinkage of the twin-gate and pin-gate samples at a dwelling time of 4 s and an injection pressure of 55 MPa.

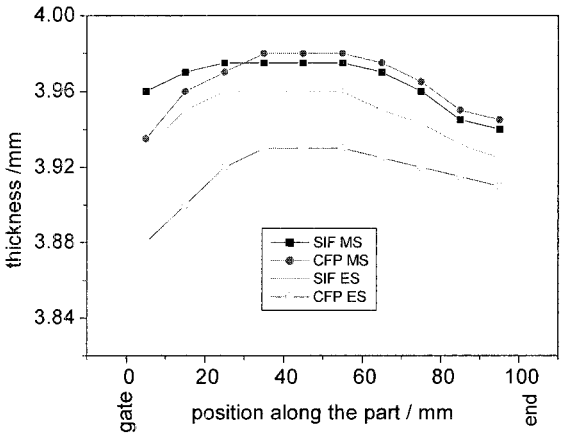

Figure 8 Thickness distribution of SIF and CFP specimens under an injection pressure of 55 MPa and at a mold temperature of 40°C and a dwelling time of 4 s.

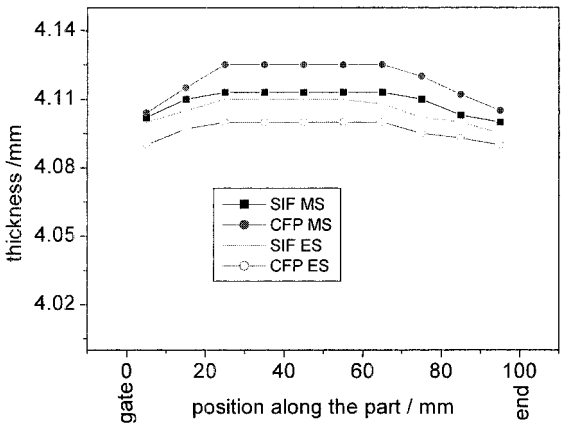

Figure 10 Thickness distribution of SIF and CFP specimens under an injection pressure of 85 MPa and at a mold temperature of 40°C and a dwelling time of 4 s.

that of the CFP samples; this is a reasonable assessment of the transverse packing efficiency produced by the transverse flow in the cavity.

Figures 8–10 show the thickness distribution along the parts under 55, 65, and 85 MPa of injection pressure, respectively. These figures clearly indicate that the differences of the thicknesses of SIF MS and SIF ES specimens are smaller than those of CFP MS and CFP ES specimens at the same positions. This signifies that the thickness distribution of the SIF samples is more uniform in the TD; in other ways, the packing efficiency of the SIF samples is higher than that of the CFP samples in the TD because of the transverse flow of the melt in the cavity with the twin gate. Figures 8–10 also demonstrate that this difference, both for SIF specimens and for CFP specimens, is becoming smaller with the increase in the pressure, as the packing efficiency is enhanced with the pressure. However, the differences of the SIF specimens are reduced to a larger extent because of the transverse flow. In the MD, near the twin gate, the SIF samples, including MS and ES specimens, have better accuracy due to less melt backflow from the cavity when the hold pressure is released because the diameters of the orifices in the twin gate are smaller than that in the pin gate. For this reason, the twin gate will produce a bigger pressure drop when a melt passes through it, and this results in a slight bigger negative error at the ends of SIF specimens under low pressure (Fig. 8) and a smaller positive error at the MS specimens under a higher pressure (Figs. 9 and 10). Moreover, the average thickness increases with the injection pressure, and this has been observed before.[26]

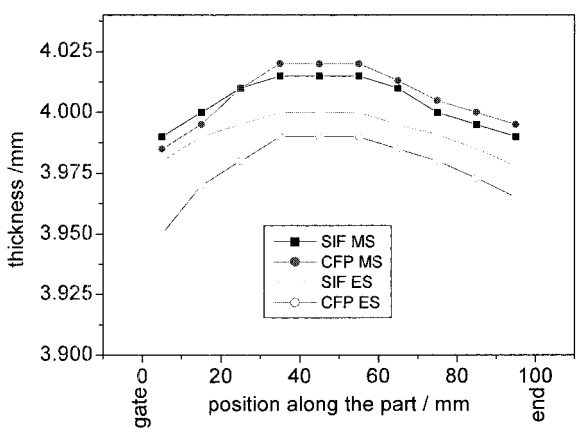

Figure 9 Thickness distribution of SIF and CFP specimens under an injection pressure of 65 MPa and at a mold temperature of 40°C and a dwelling time of 4 s.

CONCLUSIONS

SIF, which is generated with a twin gate, enhances the impact strength of injection-molded iPP parts. In the scope of this study, the impact strength of specimens molded under the condition of interference flow increases by 70–90% and changes a little with various injection pressures or mold temperatures, both in the MD and in the TD. DMTA research shows that SIF samples exhibit a higher value of E' than CFP samples. The results obtained by static and dynamic testing indicate that SIF can bring about mechanical property enhancements.

The thickness distribution of SIF samples is more uniform, and their shrinkage in the TD is smaller. These are the results brought about by SIF, and they also are indicative of the existence of a transverse flow in the cavity at the same time.

References

1. Ibar, J. P. Polym Eng Sci 1998, 38, 1.
2. Liu, C.; Manzione, L. T. Polym Eng Sci 1996, 36, 1.
3. Salloum, G.; Connolly, R.; Girard, P.; Hebert, L. P. Soc Plast Eng Annu Tech Conf Tech Pap 1990, 36, 270.

4. Mamat, A.; Trochu, F.; Sansehagrin, B. Polym Eng Sci 1995, 35, 1511.
5. Da Silva, A. N.; Tavares, M. B.; Politano, D. P.; Coutinho, F. M. B.; Rocha, M. C. G. J Appl Polym Sci 1997, 66, 2005.
6. Jafari, S. H.; Gupta, A. K. J Appl Polym Sci 1999, 71, 1153.
7. Siegmann, A. J Appl Polym Sci 1982, 27, 1053.
8. Galeski, A.; Bratczak, Z.; Pracella, M. Polymer 1984, 25, 1323.
9. Chen, X.; Guo, Q.; Mi, Y. J Appl Polym Sci 1998, 69, 1891.
10. Kodgire, P.; Kalgaonkar, R.; Hambir, S.; Bularh, N.; Jog, J. P. J Appl Polym Sci 2001, 81, 1786.
11. Guan, Q.; Zhu, X.; Shen, K. J Appl Polym Sci 1996, 62, 255.
12. Kalay, G.; Bevis, M. J. J Polym Sci Part B: Polym Phys 1997, 35, 241.
13. Ibar, J. P. Polym Commun 1983, 24, 331.
14. Kalay, G.; Allan, P. S.; Bevis, M. J. Plast Rubber Compos Process Appl 1995, 23, 71.
15. Xiaoping, W.; Yucheng, P. Suliao Gongye (in Chinese) 1996, 24(5), 32.
16. Chen, L.; Shen, K. J Appl Polym Sci 2000, 78, 1906.
17. Wenli, D.; Pengsheng, L. Chin. Pat. ZL00225780.7 (2001).
18. Tadmor, Z. J Appl Polym Sci 1974, 18, 429.
19. Han, C. D. Rheology in Polymer Processing; Academic: New York, 1976; p 284.
20. Katti, S. S.; Schultz, J. M. Polym Eng Sci 1982, 22, 1001.
21. Wenli, D.; Pengsheng, L.; et al. Chin Plast (in Chinese) 2001, 15(12), 69.
22. Wenli, D.; Pengju, W. Gaofenzi Cailiao Kexue Yu Gongcheng (in Chinese) 1995, 11(5), 97.
23. Jansen, K. M. B.; Pantani, R.; Titomanlio, G. Polym Eng Sci 1998, 38, 254.
24. Tamma, K. K.; Dowler, B. L.; Railkar, S. B. Polym Eng Sci 1988, 28, 429.
25. Santhanam, N.; Wang, K. K. Soc Plast Eng Annu Tech Conf Tech Pap 1990, 36, 270.
26. Leo, V.; Cuvelliez, C. Polym Eng Sci 1996, 36, 1916.